Molecular Therapy
Nucleic Acids
Brief Report

Phosphatidylcholine head group chemistry alters the extrahepatic accumulation of lipid-conjugated siRNA

Vignesh N. Hariharan,[1] Takahiro Nakamura,[1] Minwook Shin,[1] Qi Tang,[1] Vyankat Sontakke,[1] Jillian Caiazzi,[1] Samuel Hildebrand,[1] Anastasia Khvorova,[1] and Ken Yamada[1]

[1]RNA Therapeutics Institute, University of Massachusetts Chan Medical School, Worcester, MA 01605, USA

Small interfering RNAs (siRNAs) are revolutionizing the treatment of liver-associated indications. Yet, robust delivery to extrahepatic tissues remains a challenge. Conjugating lipids (e.g., docosanoic acid [DCA]) to siRNA supports extrahepatic delivery, but tissue accumulation remains lower than that achieved in liver by approved siRNA therapeutics. Early evidence suggests that functionalizing DCA with a head group (e.g., phosphatidylcholine [PC]) may enhance delivery to certain tissues. Here, we report the first systematic evaluation of the effect of PC head group chemistry on the extrahepatic distribution of DCA-conjugated siRNAs. We show that functionalizing DCA with a PC head group enhances siRNA accumulation in heart, muscle, lung, pancreas, duodenum, urinary bladder, and fat. Varying the size of the linker between the phosphate and choline moiety of the PC head group altered the extrahepatic accumulation of siRNA, with the optimal linker length being different for different tissues. Increasing PC head group valency also improved extrahepatic accumulation in a tissue-specific manner. This study demonstrates the structural impact of the PC moiety on the biodistribution of lipid-conjugated siRNA and introduces multiple novel PC variants for the chemical optimization of DCA-conjugated siRNA. These chemical variants can be used in the context of other lipids to increase the repertoire of conjugates for the extrahepatic distribution of siRNAs.

INTRODUCTION

Therapeutic oligonucleotides, including small interfering RNAs (siRNAs), promise to revolutionize medicine because of their informational nature, duration of effect, and potential to silence target genes previously considered "undruggable."[1] The evolution of siRNA technologies from benchtop to a clinically effective therapeutic modality depends on target specificity, chemical stability, and delivery to disease tissues, all of which are achieved through full chemical modification and conjugation.[1–6] The chemical modifications collectively form the siRNA scaffold, which can be applied, in theory, to any siRNA molecule by simply switching out one targeting sequence for another. The development of *N*-acetylgalactosamine (GalNAc)-conjugated siRNA has paved the way for multiple FDA-approved siRNA therapeutics targeting liver hepatocytes,[7] demonstrating the value of conjugation as a delivery platform. Despite these advancements in chemical engineering, the ability to deliver siRNA to extrahepatic tissues at the same levels as GalNAc-mediated hepatocyte delivery remains an outstanding problem.

One promising class of extrahepatic delivery technologies is lipid conjugation, which provides hydrophobicity-driven systemic distribution to a wide range of tissues. Lipid-conjugated siRNAs associate with plasma low- and high-density lipoproteins (LDLs and HDLs) and utilize lipoprotein transport and uptake pathways to deliver siRNA to the liver and extrahepatic tissues.[4,8,9] A diverse range of lipid conjugates have been explored in previous studies, including sterols, vitamins, saturated and unsaturated fatty acids with different chain lengths, position of the conjugate in the oligonucleotide chain as well as with and without a polar phosphatidylcholine (PC) head group.[3,10] Interestingly, the distribution profiles of siRNA conjugated to lipids with similar hydrophobicity (based on retention time in a reverse-phase high-performance liquid chromatography [HPLC] column) were different, indicating that other properties of the lipid conjugate in addition to hydrophobicity may influence tissue uptake. However, since chemical structure and hydrophobicity are interlinked, the determinants of lipid-conjugated siRNA distribution are complex and difficult to disentangle. Therefore, a systematic analysis of chemical structure is needed to understand the factors influencing tissue accumulation and identify strategies to enhance extrahepatic delivery.

In this study, we focus on modulating the chemistry of PC-docosanoic acid (PC-DCA)-conjugated siRNA. Specifically, we explore the chemical structure of the PC head group, which was previously shown to enhance placental delivery of DCA.[11] PC-DCA is currently one of the most clinically advanced lipid conjugates and is being used for placental delivery of CBP-4888, an experimental siRNA therapeutic in phase 1

Received 7 February 2024; accepted 22 May 2024;
https://doi.org/10.1016/j.omtn.2024.102230.

Correspondence: Ken Yamada, RNA Therapeutics Institute, University of Massachusetts Chan Medical School, Worcester, MA 01605, USA.
E-mail: ken.yamada@umassmed.edu

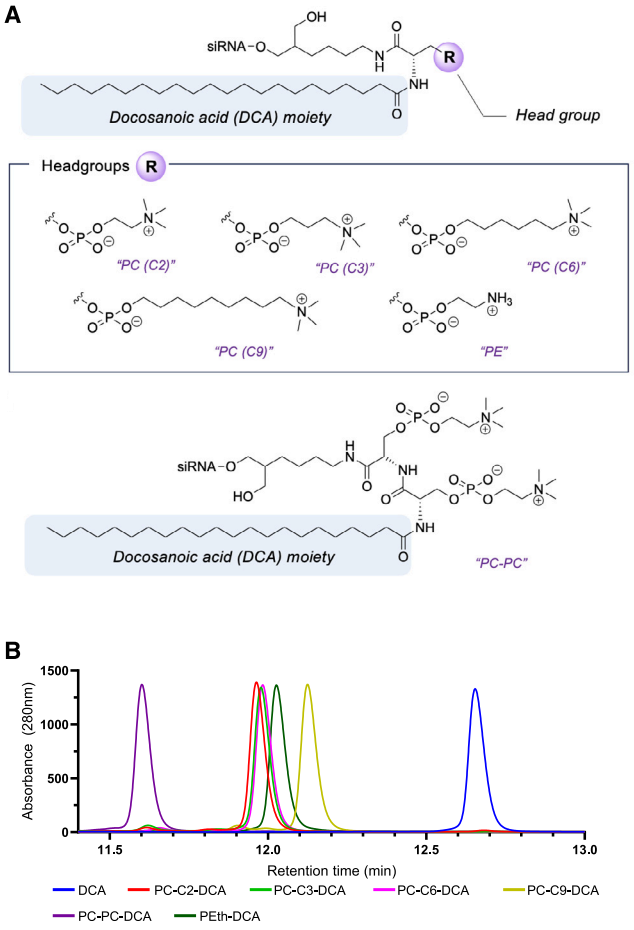

Figure 1. Head group variants can be used to alter the hydrophobicity of DCA-siRNA

(A) Schematic of conjugate head group variants used in this study and (B) high-performance liquid chromatography spectra of DCA- (blue), PC-C2-DCA- (red), PC-C3-DCA- (light green), PC-C6-DCA- (pink), PC-C9-DCA- (gold), PC-PC-DCA- (purple), and PEth-DCA-conjugated (dark green) siRNA^{htt} sense strands.

clinical trials (ClinicalTrials.gov: NCT05881993).[12–14] We sought to explore the impact of the PC head group chemistry of DCA by varying two parameters—(1) the distance between the negatively charged phosphate group and the positively charged choline group and (2) the charge-lipid ratio. We demonstrate that increasing the linker length significantly increases siRNA accumulation in extrahepatic tissues in a tissue-specific manner. We also show that increasing the charge by adding an extra PC moiety to DCA enhances accumulation in a tissue-specific manner. This work introduces head group chemistry as a novel modulator of lipid-conjugated siRNA biodistribution *in vivo*.

RESULTS

Head group variants can be used to alter the hydrophobicity of DCA-siRNA

To systematically evaluate the impact of head group chemical structure on the properties of lipid-conjugated siRNA, we synthesized DCA functionalized with variants of a single PC head group (PC-DCA).[3,11] PC-DCA variants were synthesized with ethyl (PC-C2-DCA), propyl (PC-C3-DCA), hexyl (PC-C6-DCA), or nonyl (PC-C9-DCA) linkers bridging the phosphate and choline moieties, named C2, C3, C6, and C9, respectively (Figure 1A; supplemental information). C2 is the linker used in the PC-DCA siRNAs currently being evaluated in clinical trials and reflects the structure of naturally occurring PC-lipids. All other PC-DCA variants are novel. We also synthesized PC-PC-DCA—a single DCA functionalized with two PC head groups, each with a C2 linker—and DCA functionalized with phosphatidylethanolamine (PEth), which replaces the charged trimethylammonium group of PC with a non-substituted amino group connecting to the phosphate group by the C2 linker (Figure 1A; supplemental information). All PC-DCA variants were conjugated to previously validated siRNA targeting mouse *cd47* mRNA (siRNA^{cd47}), mouse *huntingtin* mRNA (siRNA^{htt}), or a non-targeting control sequence (siRNA^{ntc}). We also conjugated non-functionalized DCA to siRNA^{cd47}, siRNA^{htt}, and siRNA^{ntc}. Mouse *cd47* and *htt* mRNAs were chosen as targets because lead siRNAs for these two genes have been previously developed and characterized by our laboratory.[15,16] These two targets are ubiquitously expressed, allowing for the measurement of gene silencing in multiple tissues.

Since hydrophobicity has traditionally been considered the determinant of systemic distribution (through plasma LDL/HDL binding), we decided to benchmark the hydrophobicity of each PC-DCA variant being tested. We analyzed sense strands of DCA siRNA^{htt} and PC-DCA siRNA^{htt} variants by reverse-phase HPLC and measured the retention times (Figure 1B). A longer retention time correlates with greater hydrophobicity. Consistent with previous reports, C2 siRNA^{htt} was less hydrophobic than non-functionalized DCA siRNA^{htt}, owing to the polar PC head group. Increasing the linker length from C2 to C3 or C6 did not significantly affect hydrophobicity. C9 siRNA^{htt} was more hydrophobic than the C2, C3, and C6 siRNA^{htt} variants but less hydrophobic than non-functionalized DCA siRNA^{htt}. PEth was less hydrophobic than C9 and only slightly more hydrophobic than C2, C3, and C6. PC-PC was the least hydrophobic of all variants tested, as expected, due to the presence of two PC head groups. Thus, this study explored a wide range of hydrophobicity in the context of the DCA conjugate.

Increasing phosphate-choline linker length promotes broad biodistribution

We next evaluated the biodistribution of DCA siRNA and the 6 PC-DCA siRNA variants in adult wild-type FVB mice. Mice were injected subcutaneously (intrascapular) with 20 mg/kg of each variant conjugated to siRNA ^{cd47}, siRNA^{htt}, or siRNA^{ntc} and were sacrificed 2 weeks post-injection. As the distribution of siRNA is sequence independent,[1] we focused on the measurement of siRNA^{cd47} in eleven tissues using the peptide nucleic acid (PNA) assay. To investigate the effect of adding a single PC head group and increasing the phosphate-choline linker length on biodistribution, we compared siRNA^{cd47} accumulation of the PC-DCA linker variants to the non-functionalized DCA conjugate. Linker variants exhibited higher accumulation in a

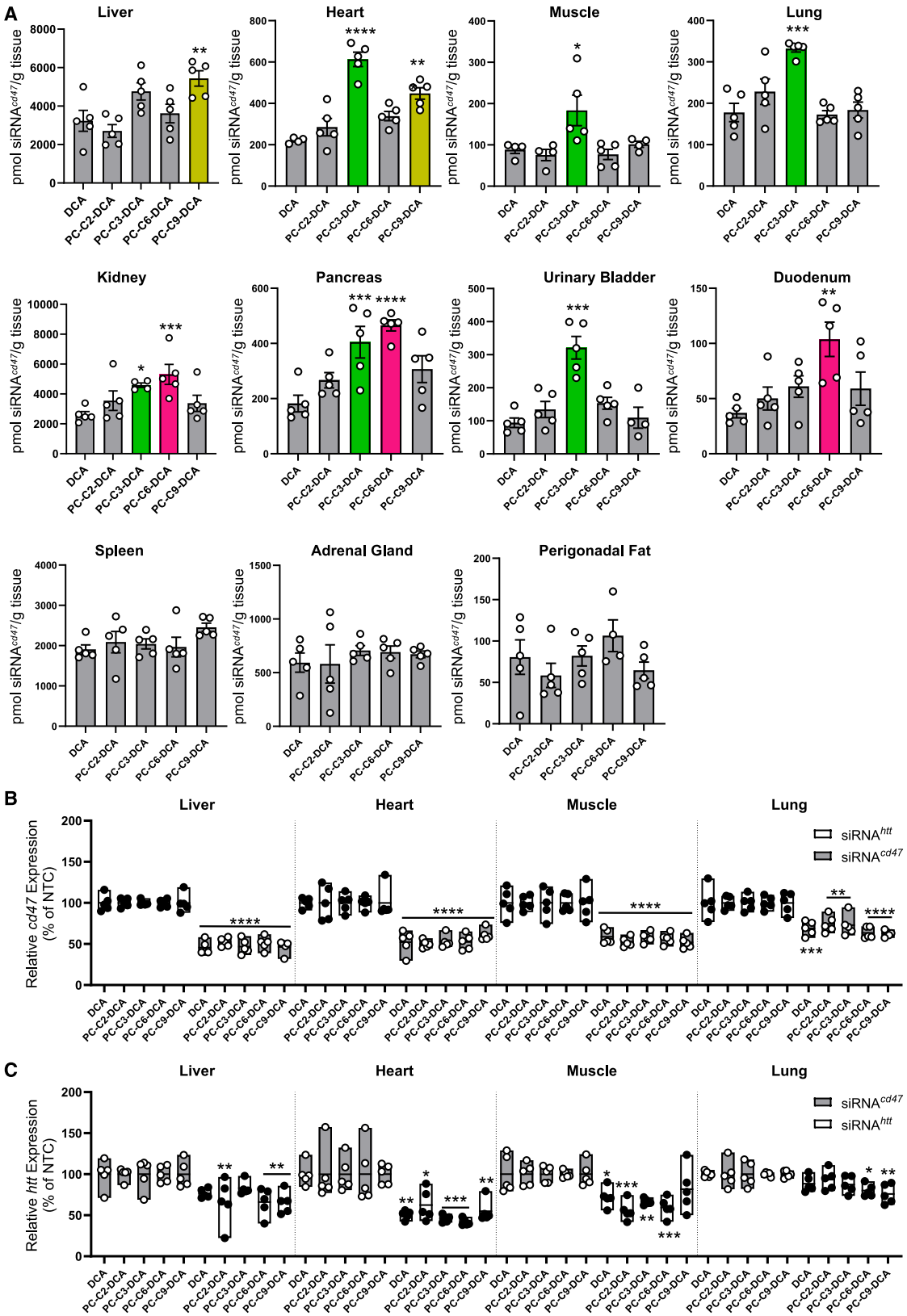

(legend on next page)

tissue-specific manner (Figure 2A). Whereas C3 was the only variant exhibiting significantly higher accumulation than DCA in muscle (183.5 vs. 88.02 pmol/g, $p < 0.05$), lung (331.7 vs. 177.6 pmol/g, $p < 0.001$), and urinary bladder (321 vs. 94 pmol/g, $p < 0.001$), C6 was the only variant that performed better than DCA in duodenum (103.7 vs. 36.9 pmol/g, $p < 0.01$). Both C3 and C6 performed better than DCA in the kidney (4,586 and 5,308 vs. 2,605 pmol/g, $p < 0.05$) and pancreas (404.5 and 465.5 vs. 181.9 pmol/g, $p < 0.001$). C3 and C9 performed better than DCA in the heart (613.2 and 448.1 vs. 220.2 pmol/g, $p < 0.001$), but only C9 performed better than DCA in the liver. The addition of the PC head group and changing the phosphate-choline linker length did not affect siRNA^{cd47} accumulation in the spleen, adrenal gland, or fat.

To explore whether the observed differences in siRNA accumulation translated into differences in siRNA efficacy, we measured *cd47* and *htt* mRNA expression in a subset of these tissues using the QuantiGene assays. DCA siRNA^{cd47} and all linker variants of PC-DCA siRNA^{cd47} significantly and similarly reduced *cd47* mRNA expression compared to siRNA^{ntc} ($p < 0.0001$ in liver, heart, and muscle; $p < 0.01$ in lung), with no significant differences among variants (Figure 2B). DCA siRNA^{htt} and linker variants of PC-DCA siRNA^{htt} also reduced *htt* mRNA expression compared to siRNA^{ntc} but did not reach statistical significance for some variants (Figure 2C), indicating perhaps that the *in vivo* potency of siRNA^{htt} is lower than that of siRNA^{cd47} and may be helpful in differentiating between the linker variants. In the liver, C2 (33.7%, $p < 0.01$), C6 (33.9%, $p < 0.01$), and C9 (34.6%, $p < 0.01$) variants produced similar levels of silencing. In the heart, maximal silencing was produced by the C3 (53.8%, $p < 0.001$) and C6 (58%, $p < 0.001$) variants. The C2 (44.5%, $p < 0.001$) and C6 (40.5%, $p < 0.001$) variants produced maximal silencing in muscle, while C9 (24.1%, $p < 0.01$) showed maximal silencing in the lung. Similar to previous reports,[3] the highest accumulation did not produce maximal silencing, indicating that some chemical variants may be internalized through unproductive pathways to initiate RNA interference (RNAi).

Increasing the valency of the PC head group affects extrahepatic tissue accumulation

In the same experiment, we evaluated siRNA accumulation of the PC-PC variant to determine the effect of increasing PC head group valency on biodistribution (Figure 3A). Variants differing in PC:lipid ratios may be found in nature and are relatively unexplored. We sought to examine the effect of doubling the PC valency on siRNA accumulation and silencing. Introducing the double PC head group did not affect siRNA^{cd47} accumulation in the liver, muscle, kidney, spleen, or adrenal gland. However, significantly higher levels of siRNA^{cd47} were found for the PC-PC variant compared to the DCA conjugate in the heart (519.8 vs. 220.2 pmol/g, $p < 0.001$), lung (341.4 vs. 177.6 pmol/g, $p < 0.001$), pancreas (565.9 vs. 181.9 pmol/g, $p < 0.0001$), urinary bladder (266.5 vs. 94 pmol/g, $p < 0.001$), duodenum (116.1 vs. 36.9 pmol/g, $p < 0.01$), and perigonadal fat (167.2 vs. 80.5 pmol/g, $p < 0.01$).

The PEth head group is a primary alkyl amine and is commonly found in plasma membrane phospholipids. The pKa of PEth is ~8.5, suggesting that the amine exists mostly in its protonated, charged form. The addition of a PEth head group did not affect siRNA^{cd47} accumulation compared to DCA in any tissue except the heart (466.6 vs. 220.2 pmol/g, $p < 0.01$) and pancreas (397.5 vs. 181.9 pmol/g, $p < 0.01$).

DCA siRNA^{cd47} and head group variants of siRNA^{cd47} significantly reduced *cd47* mRNA expression compared to siRNA^{ntc} in all tissues tested, with no significant differences between variants in heart and muscle (Figure 3B). In the liver, PEth performed significantly better than C2 (36% vs. 52% expression, $p < 0.01$), and in the lung, both PC-PC (54% expression, $p < 0.01$) and PEth (53% expression, $p < 0.01$) performed better than C2 (74% expression). PEth also outperformed DCA in the lung (53% vs. 69% expression, $p < 0.05$). DCA siRNA^{htt} and head group variants of siRNA^{htt} significantly reduced *htt* mRNA levels in the heart, muscle, and lung (Figure 3C), with no significant differences between variants in the heart. In muscle, PC-PC (47% expression, $p < 0.01$) and PEth (52% expression, $p < 0.05$) performed better than DCA (72% expression), and in the lung, PEth performed better than C2 (72% vs. 93% expression, $p < 0.01$). In the liver, *htt* mRNA expression was minimally affected, with only C2 showing statistically significant silencing compared to NTC control (66% expression, $p < 0.05$).

DISCUSSION

The evolution of oligonucleotides into a class of therapeutics was preceded by incremental innovations in chemistry that support the stability, safety, and tissue distribution of these molecules. In the field of siRNA therapeutics, the most clinically advanced delivery platform is the GalNAc conjugate, which provides receptor-targeted delivery to hepatocytes and unprecedented levels and durations of silencing in humans.[17–21] Receptor-mediated delivery to extrahepatic organs is yet to be discovered. This lacuna in the siRNA toolbox is partially compensated for by the development of hydrophobic conjugates, which allow for potentially therapeutic doses of siRNA to accumulate in extrahepatic tissues like the placenta and skeletal and cardiac

Figure 2. Increasing phosphate-choline linker length enhances extrahepatic tissue accumulation

(A) siRNA^{cd47} accumulation measured using the peptide nucleic acid hybridization assay, (B) relative cd47 mRNA expression levels measured by the QuantiGene 2.0 assay, and (C) relative htt mRNA expression levels measured by the QuantiGene 2.0 assay in various tissues of female FVB mice injected with 20 mg/kg of conjugate variants. Conjugate with the highest accumulation in each tissue represented as colored bars. Bars represent the mean ± SEM of individual animals ($n = 5$). Statistical significance was computed using one-way ANOVA with DCA as the comparator in (A) or non-targeting control (NTC) (significance marked as an asterisk [*]) and DCA (significance marked as a hash symbol [#]) as comparators in (B) and (C) with Šídák's correction for multiple comparisons (*$p < 0.05$, **$p < 0.01$, ***$p < 0.001$, and ****$p < 0.0001$). Non-significant differences have not been marked.

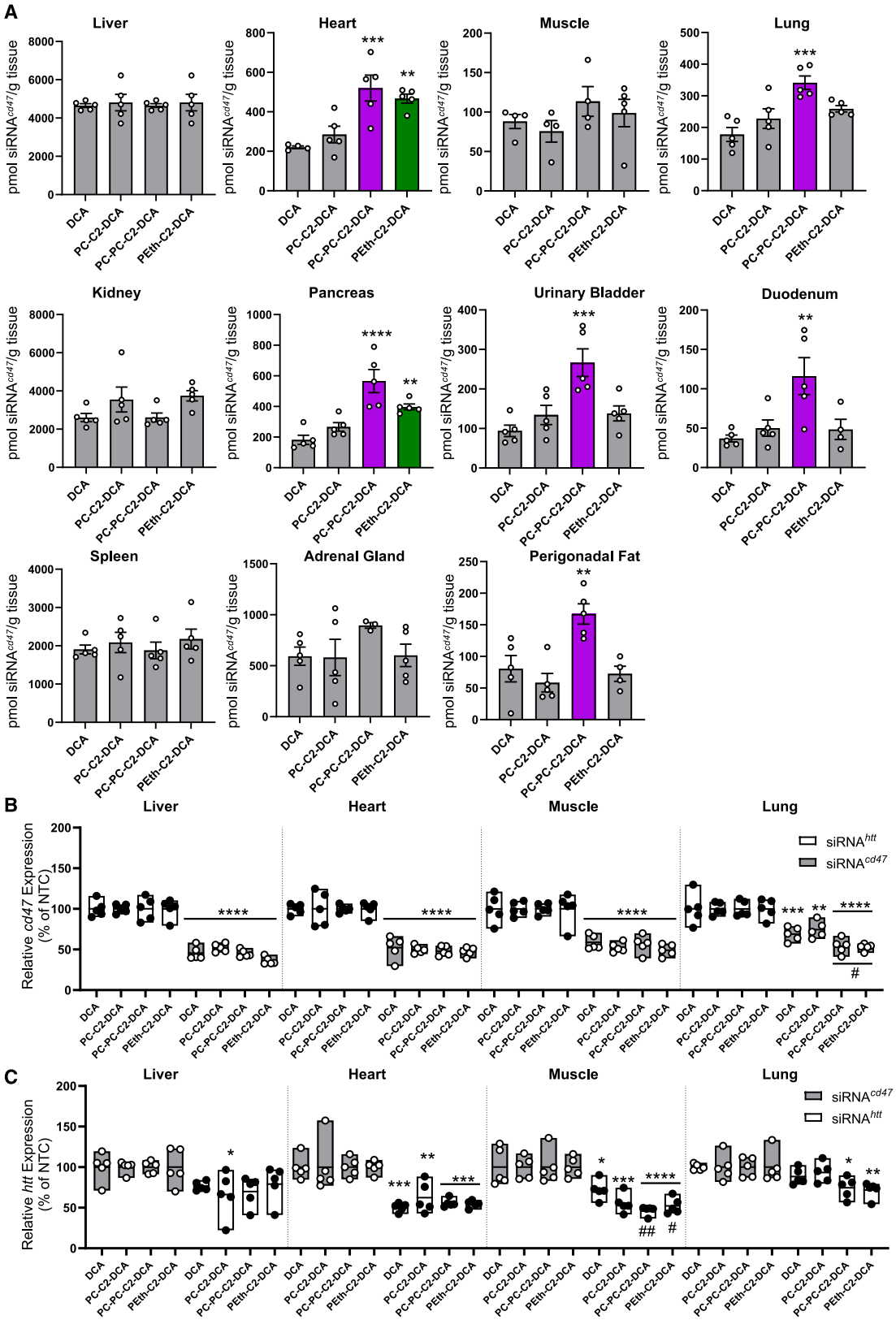

(legend on next page)

muscles after systemic administration and the skin, central nervous system, eye, and lung after local administration.[10–12,22,23] However, the functionalization of hydrophobic conjugates using charged or neutral head groups has not been systematically explored.

Here, we explored the roles of head group chemical structure and found that varying the size of the linker between the phosphate and the choline moiety from C2 (conventional) to C3, C6, or C9 was able to change the degree of siRNA accumulation in a tissue-specific manner. Interestingly, the increased accumulation was not related to the hydrophobicity of the conjugate as measured by the retention time on reverse-phase HPLC, indicating that characteristics beyond hydrophobicity may be useful in the study of lipid-conjugated siRNAs.

While this study provides empirical evidence for the role of phosphate-choline linker length in tissue accumulation, the molecular mechanisms underpinning this property remain to be explored. Changes in the affinity of conjugate variants to plasma proteins may contribute to increased circulation time and extrahepatic tissue exposure. One would expect that increased plasma residence time will result in increased extrahepatic tissue-to-liver ratios in accumulation. However, organ-to-liver ratios did not correspond to absolute siRNA concentrations for many extrahepatic tissues (Figure S34). For example, while PC-C3-DCA improved accumulation in muscle, lung, and pancreas, the organ-to-liver ratios for PC-C3-DCA were not significantly different from those of DCA for these tissues. Moreover, conjugates with similar organ-to-liver ratios had different absolute levels of siRNA in the tissue. For example, PC-C2-DCA and PC-C3-DCA had similar pancreas-to-liver ratios of 0.098 and 0.085, respectively. However, PC-C2-DCA resulted in a pancreatic accumulation of 266.5 pmol/g, while the pancreatic accumulation of PC-C3-DCA was 404.5 pmol/g (Figure S34). One possible explanation is that increased separation between the negatively charged phosphate and the positively charged choline may allow for local charge-based interactions with the extracellular matrix at each ionic pole, thereby increasing the residence time of siRNA in the tissue. However, we observed significant differences in tissue accumulation among variants with minor differences in charge separation (i.e., C2 vs. C3). Perhaps increasing the linker length increases metabolic stability against endogenous phospholipases that are known to cleave natural PC-modified phospholipids.[24] One of the other factors affecting siRNA accumulation after subcutaneous administration is injection site retention and bioavailability. We have previously shown that injection site retention of lipid-conjugated siRNAs is correlated with hydrophobicity,[3] and the degrees of injection site retention of DCA and PC-DCA are very similar. Since the hydrophobicity of the conjugate variants tested falls between the hydrophobicity of PC-C2-DCA and DCA (except for PC-PC-DCA), it is unlikely that differences in bioavailability are sufficient to explain the increases in tissue accumulation for these head group variants. Future work should determine how accumulation is affected by replacing the charged choline group with a neutral butyl group and/or replacing the DCA with other hydrophobic conjugates like palmitic acid (C16) and myristic acid (C14) to fully explore the utility of conjugate head groups. It should be noted that while increased accumulation was observed in multiple tissues, target silencing measured at 2 weeks post-injection did not correlate with the accumulation increase. Previously, we have shown that the effect of increased accumulation of siRNA is apparent in the duration of the effect but not in short-term efficacy. Regions with higher siRNA accumulation did not show greater gene silencing in the short term, but the duration of target silencing was prolonged compared to regions with lower siRNA accumulation.[25] This is probably because short-term silencing is limited by Ago2 expression levels, target mRNA accessibility, and competition with endogenous Ago2 substrates,[26–28] while the presence of endosomal depots of siRNA enables continuous RNAi activity over time and leads to a prolonged duration of effect.[29,30] Therefore, the increased siRNA accumulation seen in this study may not show improved efficacy in the short term due to limited Ago2 availability but may be productive for long-term silencing through endosomal leakage. A second explanation for the lack of short-term efficacy improvement may be that the modified PC head groups interfere with RNA-induced silencing complex (RISC) loading of the siRNA duplex. However, we have previously shown that lipid conjugation of siRNA does not affect RISC cleavage rates.[31] Additionally, in the present study, we have used previously reported cleavable deoxythymidine linkers between the sense strand and the conjugate to limit the interference of the conjugate with Ago2 loading post-internalization.[32] Therefore, the lack of short-term efficacy is likely not due to steric hinderance from the conjugate. Future studies should investigate the optimal duration and dosing at which correlates of accumulation and target silencing become more apparent.

Overall, this study provides evidence that the PC head group can greatly enhance broad extrahepatic delivery of the DCA conjugate. Among the variants tested, PC-C3-DCA was the best-performing conjugate with maximal accumulation in a broad range of tissues. However, we believe that there is potential for further chemical optimization by exploring different kinds of head groups as well as different kinds of lipid conjugates. Head group modulation could serve as a novel strategy to modulate pharmacokinetics in the context

Figure 3. Increasing the valency of PC head group affects accumulation in some tissues

(A) siRNA^{cd47} accumulation measured using the peptide nucleic acid hybridization assay, (B) relative cd47 mRNA expression levels measured by the QuantiGene 2.0 assay, and (C) relative htt mRNA expression levels measured by the QuantiGene 2.0 assay in various tissues of female FVB mice injected with 20 mg/kg of conjugate variants. Conjugate with the highest accumulation in each tissue is represented as colored bars. Bars represent the mean ± SEM of individual animals (n = 5). Statistical significance computed using one-way ANOVA with DCA as the comparator in (A) or NTC (significance marked as an asterisk [*]) and DCA (significance marked as a hash symbol [#]) as comparators in (B) and (C) with Šídák's correction for multiple comparisons (* or #$p < 0.05$, ** or ##$p < 0.01$, ***$p < 0.001$, and ****$p < 0.0001$). Non-significant differences have not been marked.

of hydrophobically conjugated siRNA. Additionally, while the conjugates tested in this study were tolerated at the dose administered, future work should include toxicology intended to characterize the safety profile of lead conjugates and the consequences of enhanced tissue accumulation on the therapeutic index of the siRNA.

MATERIALS AND METHODS

General methods for oligonucleotide synthesis, deprotection, and purification

Oligonucleotides were synthesized using standard phosphoramidite-based solid-phase synthesis, deprotected, and purified by HPLC. Custom-made lipid-functionalized controlled pore glass (CPG) was used for the synthesis of sense strands (see supplemental information; Figures S1–S5). Antisense strands were synthesized on UnyLinker-functionalized CPG (ChemGenes). Standard deprotection and cleavage conditions specific to sense strands or antisense strands were used. All siRNAs synthesized were fully modified with 2′-O-methyl or 2′-fluoro groups, phosphorothioate backbones in the termini, and 5'-(*E*)-vinylphosphonate on the antisense strand. Oligonucleotides were purified by standard HPLC methods specific to sense and antisense strands. The identity of custom synthesized lipid conjugate precursors was verified using nuclear magnetic resonance and LC-mass spectrometry (MS), and the identity and quality of synthesized oligonucleotides were verified using LC-MS (Figures S6–S33).

Animal administrations

All animal experiments were conducted in accordance with the guidelines of the University of Massachusetts Chan Medical School (UMass Chan) Institutional Animal Care and Use Committee (IACUC). All procedures were performed as approved under IACUC protocol #A-2411. Female wild-type FVB mice were purchased from The Jackson Laboratory (Bar Harbor, ME, USA). Mice were 6–8 weeks old at the time of the experiments. The mice were divided into 14 groups with five mice per group and injected with siRNA variants formulated in phosphate-buffered saline and administered in a volume of 150 μL subcutaneously between the shoulder blades. siRNA variants included siRNA^{htt} and siRNA^{cd47} sequences synthesized with one of the following 7 conjugates: DCA, PC-C2-DCA, PC-C3-DCA, PC-C6-DCA, PC-C9-DCA, PC-PC-C2-DCA or PEth-C2-DCA. Animals were terminated at 2 weeks post-injection, and the liver, heart, muscle, lung, kidney, pancreas, urinary bladder, duodenum, spleen, adrenal gland, and perigonadal fat tissue were collected and immersed in RNAlater (Thermo Fisher Scientific) solution as per the manufacturer's recommendations. Mice were housed in pathogen-free animal facilities at UMass Chan with a 12 h/12 h light/dark cycle, controlled temperature (23°C ± 1°C), humidity (50% ± 20%), and *ad libitum* food and water.

PNA hybridization assay

Quantification of antisense strand accumulation in tissues was performed by the PNA hybridization assay as previously described. Briefly, ∼0.2-7 mg of tissue was weighed and lysed in QuantiGene Homogenizing Solution (Invitrogen) containing 0.2 mg/mL Ambion Recombinant Proteinase K Solution (Invitrogen) using the TissueLyser II (Qiagen) and 3 mm Tungsten Carbide Beads (Qiagen) and incubated at 65°C for half an hour. Following incubation, tissue lysates were treated with 3M potassium chloride to precipitate sodium dodecyl sulfate and pelleted by centrifugation at 4,000 × *g* for 15 min. Supernatants were hybridized with Cy3-labeled PNA probes (PNABio, Thousand Oaks, CA, USA) fully complementary to the siRNA^{cd47} antisense strand and analyzed by HPLC (Agilent, Santa Clara, CA, USA) over a DNAPac PA100 anion-exchange column (Thermo Fisher Scientific). Cy3 fluorescence was monitored, and peaks were integrated using a custom python script. Final concentrations of siRNA^{cd47} in tissue lysate were determined using a standard curve generated from samples containing known concentrations of siRNA^{cd47}.

QuantiGene Singleplex 2.0 (bDNA) assay

Tissue lysates prepared in the same manner as above (see PNA hybridization assay) were used to measure *htt* and *cd47* mRNA levels using the QuantiGene Singleplex assay kit (Invitrogen) with the following probe sets, mouse *htt* (SB-14150), mouse *cd47* (SB-3029698), and mouse *hprt* (SB-15463), according to the manufacturer's instructions. siRNA^{htt}-treated animals were used as the non-targeting control for the normalization of *cd47* expression levels, and siRNA^{cd47}-treated animals were used as the non-targeting control for the normalization of *htt* expression levels.

DATA AND CODE AVAILABILITY

All data generated from this study have been made available in this manuscript.

SUPPLEMENTAL INFORMATION

Supplemental information can be found online at https://doi.org/10.1016/j.omtn.2024.102230.

ACKNOWLEDGMENTS

We thank all members of the Khvorova lab for their helpful discussions and support. This work was supported by the National Institutes of Health grants R01 HD086111, S10 OD020012, and R35 GM131839 and a subaward from the University of Oxford (UoA TransNAT award MR/X008029/1).

AUTHOR CONTRIBUTIONS

V.N.H., T.N., A.K., and K.Y. designed the study; T.N. and K.Y. designed lipid conjugate structures and T.N. synthtesized all lipid conjugate variants and oligonucleotides, and V.S. conducted scale-up synthesis of PEth-DCA solid support. V.N.H., T.N., M.S., Q.T., J.C., and S.H. performed the in vivo experiments and data analysis; V.N.H., A.K., and K.Y. wrote the manuscript.

DECLARATION OF INTERESTS

The University of Massachusetts Chan Medical School has filed a patent application for the novel conjugates described here. A.K. discloses ownership of stocks in RXi Pharmaceuticals and Advirna and is a founder of Atalanta Therapeutics and Comanche Biopharma.

V.N.H. is an employee of Comanche Biopharma and owns stock options.

REFERENCES

1. Khvorova, A., and Watts, J.K. (2017). The chemical evolution of oligonucleotide therapies of clinical utility. Nat. Biotechnol. *35*, 238–248.
2. Jackson, A.L., Burchard, J., Leake, D., Reynolds, A., Schelter, J., Guo, J., Johnson, J.M., Lim, L., Karpilow, J., Nichols, K., et al. (2006). Position-specific chemical modification of siRNAs reduces "off-target" transcript silencing. RNA *12*, 1197–1205.
3. Biscans, A., Coles, A., Haraszti, R., Echeverria, D., Hassler, M., Osborn, M., and Khvorova, A. (2019). Diverse lipid conjugates for functional extra-hepatic siRNA delivery in vivo. Nucleic Acids Res. *47*, 1082–1096.
4. Osborn, M.F., and Khvorova, A. (2018). Improving siRNA Delivery In Vivo Through Lipid Conjugation. Nucleic Acid Ther. *28*, 128–136.
5. Parmar, R., Willoughby, J.L.S., Liu, J., Foster, D.J., Brigham, B., Theile, C.S., Charisse, K., Akinc, A., Guidry, E., Pei, Y., et al. (2016). 5'-(E)-Vinylphosphonate: A Stable Phosphate Mimic Can Improve the RNAi Activity of siRNA-GalNAc Conjugates. Chembiochem *17*, 985–989.
6. Eckstein, F. (2014). Phosphorothioates, essential components of therapeutic oligonucleotides. Nucleic Acid Ther. *24*, 374–387.
7. Springer, A.D., and Dowdy, S.F. (2018). GalNAc-siRNA Conjugates: Leading the Way for Delivery of RNAi Therapeutics. Nucleic Acid Ther. *28*, 109–118.
8. Osborn, M.F., Coles, A.H., Biscans, A., Haraszti, R.A., Roux, L., Davis, S., Ly, S., Echeverria, D., Hassler, M.R., Godinho, B.M.D.C., et al. (2019). Hydrophobicity drives the systemic distribution of lipid-conjugated siRNAs via lipid transport pathways. Nucleic Acids Res. *47*, 1070–1081.
9. Wolfrum, C., Shi, S., Jayaprakash, K.N., Jayaraman, M., Wang, G., Pandey, R.K., Rajeev, K.G., Nakayama, T., Charrise, K., Ndungo, E.M., et al. (2007). Mechanisms and optimization of in vivo delivery of lipophilic siRNAs. Nat. Biotechnol. *25*, 1149–1157.
10. Brown, K.M., Nair, J.K., Janas, M.M., Anglero-Rodriguez, Y.I., Dang, L.T.H., Peng, H., Theile, C.S., Castellanos-Rizaldos, E., Brown, C., Foster, D., et al. (2022). Expanding RNAi therapeutics to extrahepatic tissues with lipophilic conjugates. Nat. Biotechnol. *40*, 1500–1508.
11. Davis, S.M., Hariharan, V.N., Lo, A., Turanov, A.A., Echeverria, D., Sousa, J., McHugh, N., Biscans, A., Alterman, J.F., Karumanchi, S.A., et al. (2022). Chemical optimization of siRNA for safe and efficient silencing of placental sFLT1. Mol. Ther. Nucleic Acids *29*, 135–149.
12. Biscans, A., Caiazzi, J., McHugh, N., Hariharan, V., Muhuri, M., and Khvorova, A. (2021). Docosanoic acid conjugation to siRNA enables functional and safe delivery to skeletal and cardiac muscles. Mol. Ther. *29*, 1382–1394.
13. Sakowicz, A., Bralewska, M., Rybak-Krzyszkowska, M., Grzesiak, M., and Pietrucha, T. (2023). New Ideas for the Prevention and Treatment of Preeclampsia and Their Molecular Inspirations. Int. J. Mol. Sci. *24*, 12100.
14. Park, B. (2023). Novel siRNA Therapy Fast Tracked for Preeclampsia Treatment. MPR Monthly Prescribing Reference.
15. Hariharan, V.N., Shin, M., Chang, C.W., O'Reilly, D., Biscans, A., Yamada, K., Guo, Z., Somasundaran, M., Tang, Q., Monopoli, K., et al. (2023). Divalent siRNAs are bioavailable in the lung and efficiently block SARS-CoV-2 infection. Proc. Natl. Acad. Sci. USA *120*, e2219523120.
16. Alterman, J.F., Hall, L.M., Coles, A.H., Hassler, M.R., Didiot, M.C., Chase, K., Abraham, J., Sottosanti, E., Johnson, E., Sapp, E., et al. (2015). Hydrophobically Modified siRNAs Silence Huntingtin mRNA in Primary Neurons and Mouse Brain. Mol. Ther. Nucleic Acids *4*, e266.
17. Hoy, S.M. (2018). Patisiran: First Global Approval. Drugs *78*, 1625–1631.
18. Scott, L.J. (2020). Givosiran: First Approval. Drugs *80*, 335–339.
19. Scott, L.J., and Keam, S.J. (2021). Lumasiran: First Approval. Drugs *81*, 277–282.
20. Lamb, Y.N. (2021). Inclisiran: First Approval. Drugs *81*, 389–395.
21. Mullard, A. (2022). FDA approves fifth RNAi drug - Alnylam's next-gen hATTR treatment. Nat. Rev. Drug Discov. *21*, 548–549.
22. Tang, Q., Fakih, H.H., Zain Ui Abideen, M., Hildebrand, S.R., Afshari, K., Gross, K.Y., Sousa, J., Maebius, A.S., Bartholdy, C., Søgaard, P.P., et al. (2023). Rational design of a JAK1-selective siRNA inhibitor for the modulation of autoimmunity in the skin. Nat. Commun. *14*, 7099.
23. Tang, Q., Sousa, J., Echeverria, D., Fan, X., Hsueh, Y.C., Afshari, K., MeHugh, N., Cooper, D.A., Vangjeli, L., Monopoli, K., et al. (2022). RNAi-based modulation of IFN-gamma signaling in skin. Mol. Ther. *30*, 2709–2721.
24. Gomez-Cambronero, J. (2014). Phospholipase D in cell signaling: from a myriad of cell functions to cancer growth and metastasis. J. Biol. Chem. *289*, 22557–22566.
25. Alterman, J.F., Godinho, B.M.D.C., Hassler, M.R., Ferguson, C.M., Echeverria, D., Sapp, E., Haraszti, R.A., Coles, A.H., Conroy, F., Miller, R., et al. (2019). A divalent siRNA chemical scaffold for potent and sustained modulation of gene expression throughout the central nervous system. Nat. Biotechnol. *37*, 884–894.
26. Vickers, T.A., Lima, W.F., Nichols, J.G., and Crooke, S.T. (2007). Reduced levels of Ago2 expression result in increased siRNA competition in mammalian cells. Nucleic Acids Res. *35*, 6598–6610.
27. Grimm, D., Streetz, K.L., Jopling, C.L., Storm, T.A., Pandey, K., Davis, C.R., Marion, P., Salazar, F., and Kay, M.A. (2006). Fatality in mice due to oversaturation of cellular microRNA/short hairpin RNA pathways. Nature *441*, 537–541.
28. Didiot, M.C., Ferguson, C.M., Ly, S., Coles, A.H., Smith, A.O., Bicknell, A.A., Hall, L.M., Sapp, E., Echeverria, D., Pai, A.A., et al. (2018). Nuclear Localization of Huntingtin mRNA Is Specific to Cells of Neuronal Origin. Cell Rep. *24*, 2553–2560.e5.
29. Brown, C.R., Gupta, S., Qin, J., Racie, T., He, G., Lentini, S., Malone, R., Yu, M., Matsuda, S., Shulga-Morskaya, S., et al. (2020). Investigating the pharmacodynamic durability of GalNAc-siRNA conjugates. Nucleic Acids Res. *48*, 11827–11844.
30. Dowdy, S.F., Setten, R.L., Cui, X.S., and Jadhav, S.G. (2022). Delivery of RNA Therapeutics: The Great Endosomal Escape. Nucleic Acid Ther. *32*, 361–368.
31. Hassler, M.R., Turanov, A.A., Alterman, J.F., Haraszti, R.A., Coles, A.H., Osborn, M.F., Echeverria, D., Nikan, M., Salomon, W.E., Roux, L., et al. (2018). Comparison of partially and fully chemically-modified siRNA in conjugate-mediated delivery in vivo. Nucleic Acids Res. *46*, 2185–2196.
32. Biscans, A., Caiazzi, J., Davis, S., McHugh, N., Sousa, J., and Khvorova, A. (2020). The chemical structure and phosphorothioate content of hydrophobically modified siRNAs impact extrahepatic distribution and efficacy. Nucleic Acids Res. *48*, 7665–7680.